MOTION-BASED FIGURE-GROUND SEGMENTATION BY MAXIMUM MOTION SEPARATION

Abdol-Reza Mansouri†*, Amar Mitiche, and Fabien Dolla*

INRS-Télécommunications, Institut National de la Recherche Scientifique
Place Bonaventure, Suite 6900, Montréal, Québec, Canada, H5A 1K6
† Division of Engineering and Applied Sciences, Harvard University
Cambridge, MA 02138

1. PROBLEM STATEMENT

Motion-based image segmentation is one of the basic problems of image processing and computer vision, with numerous applications to object based image coding (such as in MPEG-4) and computer vision (image interpretation and scene analysis). Various approaches to motion-based image segmentation with level sets have already been proposed, but most fall in the category of motion detection and impose severe constraints on the image sequence (e.g., moving object on a fixed background) [1], [3]. Those that perform true motion-based segmentation on the other hand, require that the motion parameters be computed prior to the segmentation [2].

In this paper, we propose a novel algorithm for motion-based figure-ground segmentation that extends the functional proposed by Yezzi [5] for intensity-based image segmentation. Our proposed algorithm is expressed as the solution of level set partial differential equations [4], and the desired motion-based segmentation is then obtained as the zero level set obtained at convergence of the evolution. The method allows camera movement, in which case both the figure and ground can be moving. The computed segmentation yields two regions, for figure and ground, with maximally separated motions.

The main benefit of our proposed algorithm is that contrary to existing motion-based segmentation algorithms that use level sets, it does not require that the motion parameters be computed prior to the segmentation; rather, these parameters are computed in parallel with the segmentation and even guide the latter. We detail our algorithm and illustrate its performance with translational motion. Very promising preliminary results are obtained on real image sequences with synthetic motion.

2. MOTION-BASED SEGMENTATION VIA LEVEL SET PDES

2.1. Basic Models and Functionals

Let I be an image sequence defined over the spatio-temporal domain $\boldsymbol{D} = \Omega \times [0, T]$, where Ω is a bounded open subset of $\mathbb{R}^2$ representing the domain of each image in the sequence, and $[0, T]$ is the time interval of the sequence. Assume that the (connected or disconnected) region $\boldsymbol{R} \subset \Omega$ undergoes translational motion with translation vector $\vec{u}(\boldsymbol{R})$, while its complement $\boldsymbol{R}^c$ (the background) undergoes motion with translation vector $\vec{u}(\boldsymbol{R}^c)$. The constraint of constancy of intensity along motion trajectories can be written:

$$\frac{dI}{dt} = 0$$

leading to the equations

$$\begin{aligned} \vec{\nabla} I(\boldsymbol{x}) \cdot \vec{u}(\boldsymbol{R}) + I_t(\boldsymbol{x}) = 0, \quad \forall \boldsymbol{x} \in \boldsymbol{R}, \\ \vec{\nabla} I(\boldsymbol{x}) \cdot \vec{u}(\boldsymbol{R}^c) + I_t(\boldsymbol{x}) = 0, \quad \forall \boldsymbol{x} \in \boldsymbol{R}^c, \end{aligned}$$

where $\nabla I = (I_x, I_y)$ is the spatial gradient of I, "$\cdot$" denotes the Euclidean inner product, and I_t is the the temporal derivative of I. The translation vectors $\vec{u}(\boldsymbol{R})$ and $\vec{u}(\boldsymbol{R}^c)$ can then be computed as solutions to the following respective minimization problems:

$$\begin{aligned} \vec{u}(\boldsymbol{R}) &= \arg\min_{\vec{u} \in \mathbb{R}^2} \int_{\boldsymbol{R}} (\vec{\nabla} I(\boldsymbol{x}) \cdot \vec{u} + I_t(\boldsymbol{x}))^2 d\boldsymbol{x}, \\ \vec{u}(\boldsymbol{R}^c) &= \arg\min_{\vec{u} \in \mathbb{R}^2} \int_{\boldsymbol{R}^c} (\vec{\nabla} I(\boldsymbol{x}) \cdot \vec{u} + I_t(\boldsymbol{x}))^2 d\boldsymbol{x}, \end{aligned}$$

leading to the following necessary conditions:

$$\begin{aligned} u_1(\boldsymbol{R}) \int_{\boldsymbol{R}} (I_x)^2 + u_2(\boldsymbol{R}) \int_{\boldsymbol{R}} I_x I_y + \int_{\boldsymbol{R}} I_x I_t &= 0, \\ u_1(\boldsymbol{R}) \int_{\boldsymbol{R}} I_x I_y + u_2(\boldsymbol{R}) \int_{\boldsymbol{R}} (I_y)^2 + \int_{\boldsymbol{R}} I_y I_t &= 0, \\ u_1(\boldsymbol{R}^c) \int_{\boldsymbol{R}^c} (I_x)^2 + u_2(\boldsymbol{R}^c) \int_{\boldsymbol{R}^c} I_x I_y + \int_{\boldsymbol{R}^c} I_x I_t &= 0, \\ u_1(\boldsymbol{R}^c) \int_{\boldsymbol{R}^c} I_x I_y + u_2(\boldsymbol{R}^c) \int_{\boldsymbol{R}^c} (I_y)^2 + \int_{\boldsymbol{R}^c} I_y I_t &= 0, \end{aligned}$$

where $\vec{u} = (u_1, u_2)$. Finally, we obtain the following expressions for $\vec{u}(\boldsymbol{R})$ and $\vec{u}(\boldsymbol{R}^c)$ from these necessary conditions:

$$\begin{aligned} u_1(\boldsymbol{R}) &= \frac{-\int_{\boldsymbol{R}} (I_y)^2 \int_{\boldsymbol{R}} I_x I_t + \int_{\boldsymbol{R}} I_x I_y \int_{\boldsymbol{R}} I_y I_t}{\int_{\boldsymbol{R}} (I_x)^2 \int_{\boldsymbol{R}} (I_y)^2 - (\int_{\boldsymbol{R}} I_x I_y)^2}, \\ u_2(\boldsymbol{R}) &= \frac{\int_{\boldsymbol{R}} I_x I_y \int_{\boldsymbol{R}} I_x I_t - \int_{\boldsymbol{R}} (I_x)^2 \int_{\boldsymbol{R}} I_y I_t}{\int_{\boldsymbol{R}} (I_x)^2 \int_{\boldsymbol{R}} (I_y)^2 - (\int_{\boldsymbol{R}} I_x I_y)^2}, \\ u_1(\boldsymbol{R}^c) &= \frac{-\int_{\boldsymbol{R}^c} (I_y)^2 \int_{\boldsymbol{R}^c} I_x I_t + \int_{\boldsymbol{R}^c} I_x I_y \int_{\boldsymbol{R}^c} I_y I_t}{\int_{\boldsymbol{R}^c} (I_x)^2 \int_{\boldsymbol{R}^c} (I_y)^2 - (\int_{\boldsymbol{R}^c} I_x I_y)^2}, \\ u_2(\boldsymbol{R}^c) &= \frac{\int_{\boldsymbol{R}^c} I_x I_y \int_{\boldsymbol{R}^c} I_x I_t - \int_{\boldsymbol{R}^c} (I_x)^2 \int_{\boldsymbol{R}^c} I_y I_t}{\int_{\boldsymbol{R}^c} (I_x)^2 \int_{\boldsymbol{R}^c} (I_y)^2 - (\int_{\boldsymbol{R}^c} I_x I_y)^2}, \end{aligned}$$

This work was supported by the Natural Sciences and Engineering Research Council of Canada under Strategic Grant STR224122.

In Proc. ICIP 2003, Sept. 14-17, 2003, Barcelona, Spain

Following Yezzi [5], we consider the following minimization problem:

$$\boldsymbol{R}^\star = \arg\min_{\boldsymbol{R}\subset\Omega} -\frac{1}{2}\|\vec{u}(\boldsymbol{R}) - \vec{u}(\boldsymbol{R}^c)\|^2$$

In other words, we wish to compute the region $\boldsymbol{R} \subset \Omega$ such that the average translational motion within $\boldsymbol{R}$ is maximally separated from the average translational motion outside of $\boldsymbol{R}$. The desired motion-based segmentation of the image is obtained as the solution to this minimization problem.

2.2. Curve evolution equations

Let $\vec{\gamma} : [0,1] \to \mathbb{R}^2$ be the estimator of the oriented boundary $\partial\boldsymbol{R}$ of $\boldsymbol{R}$. Let $\boldsymbol{R}_{\vec{\gamma}}$ be the region inside of $\vec{\gamma}$, and $\boldsymbol{R}^c_{\vec{\gamma}}$ the region outside of $\vec{\gamma}$. The motion-based segmentation problem can then be formulated as the following minimization problem, to determine an estimate of $\vec{\gamma}$ that corresponds to a maximum separation between the motion of the region inside and the motion of the region outide:

$$\vec{\gamma}^\star = \arg\min_{\vec{\gamma}:[0,1]\to\mathbb{R}^2} -\frac{1}{2}\|\vec{u}(\boldsymbol{R}_{\vec{\gamma}}) - \vec{u}(\boldsymbol{R}^c_{\vec{\gamma}})\|^2$$

The minimization of the functional $\vec{\gamma} \mapsto -\frac{1}{2}\|\vec{u}(\boldsymbol{R}_{\vec{\gamma}}) - \vec{u}(\boldsymbol{R}^c_{\vec{\gamma}})\|^2$ is performed by embedding the curve $\vec{\gamma} : [0,1] \to \mathbb{R}^2$ in a one-parameter family $\vec{\gamma} : [0,1] \times \mathbb{R}^+ \to \mathbb{R}^2$ of plane curves such that $\vec{\gamma}(.,\infty) = \lim_{\tau\to\infty} \vec{\gamma}(.,\tau)$ be a minimum of $\frac{1}{2}\|\vec{u}(\boldsymbol{R}_{\vec{\gamma}}) - \vec{u}(\boldsymbol{R}^c_{\vec{\gamma}})\|^2$. Such a family is constructed by prescribing the evolution of $\vec{\gamma}$ according to the following Euler-Lagrange descent equation:

$$\begin{aligned}\frac{d\vec{\gamma}(s,\tau)}{d\tau} &= \frac{1}{2}\frac{\partial}{\partial\vec{\gamma}}\|\vec{u}(\boldsymbol{R}_{\vec{\gamma}}) - \vec{u}(\boldsymbol{R}^c_{\vec{\gamma}})\|^2 \\ &= <\vec{u}(\boldsymbol{R}_{\vec{\gamma}}) - \vec{u}(\boldsymbol{R}^c_{\vec{\gamma}}), \frac{\partial\vec{u}(\boldsymbol{R}_{\vec{\gamma}})}{\partial\vec{\gamma}} - \frac{\partial\vec{u}(\boldsymbol{R}^c_{\vec{\gamma}})}{\partial\vec{\gamma}}>,\end{aligned}$$

where $< .,. >$ is the Euclidean inner product, and $\frac{\partial}{\partial\vec{\gamma}}$ is the functional derivative with respect to $\vec{\gamma}$. The desired segmentation is then given by the partition $\{\boldsymbol{R}_{\vec{\gamma}(.,\infty)}, \boldsymbol{R}^c_{\vec{\gamma}(.,\infty)}\}$ of Ω. Note that an alternative functional could be considered as well [5] by including a prior term on regions favoring regions with smaller perimeter. This leads to the following energy minimization problem

$$\vec{\gamma}^\star = \arg\min_{\vec{\gamma}:[0,1]\to\mathbb{R}^2} -\frac{1}{2}\|\vec{u}(\boldsymbol{R}_{\vec{\gamma}}) - \vec{u}(\boldsymbol{R}^c_{\vec{\gamma}})\|^2 + \lambda\int_{\vec{\gamma}} ds,$$

with λ a positive constant (ds being the element of arc length), and to the following curve evolution equation:

$$\begin{aligned}\frac{d\vec{\gamma}(s,\tau)}{d\tau} &= \frac{1}{2}\frac{\partial}{\partial\vec{\gamma}}\|\vec{u}(\boldsymbol{R}_{\vec{\gamma}}) - \vec{u}(\boldsymbol{R}^c_{\vec{\gamma}})\|^2 - \lambda\frac{\partial}{\partial\vec{\gamma}}\int_{\vec{\gamma}} ds \\ &= <\vec{u}(\boldsymbol{R}_{\vec{\gamma}}) - \vec{u}(\boldsymbol{R}^c_{\vec{\gamma}}), \frac{\partial\vec{u}(\boldsymbol{R}_{\vec{\gamma}})}{\partial\vec{\gamma}} - \frac{\partial\vec{u}(\boldsymbol{R}^c_{\vec{\gamma}})}{\partial\vec{\gamma}}> \\ &\quad -\lambda\kappa\vec{N}, \qquad (1)\end{aligned}$$

where κ is the curvature of $\vec{\gamma}$ and $\vec{N}$ the outward unit normal to $\vec{\gamma}$. The inclusion of this prior term has a regularizing effect on the segmentation, leading to regions with smoother boundaries. A straightforward (but tedious) computation shows that the functional derivative $\frac{\partial\vec{u}(\boldsymbol{R}_{\vec{\gamma}})}{\partial\vec{\gamma}}$ of $\vec{u}(\boldsymbol{R}_{\vec{\gamma}})$ with respect to $\vec{\gamma}$ is vector in $\boldsymbol{R}^2$ having respectively components:

$$\frac{\partial u_1(\boldsymbol{R}_{\vec{\gamma}})}{\partial\vec{\gamma}} = \frac{P_1'Q - P_1Q'}{(\int_{\boldsymbol{R}_{\vec{\gamma}}}(I_x)^2\int_{\boldsymbol{R}_{\vec{\gamma}}}(I_y)^2 - (\int_{\boldsymbol{R}_{\vec{\gamma}}} I_xI_y)^2)^2}\vec{N} \qquad (2)$$

and

$$\frac{\partial u_2(\boldsymbol{R}_{\vec{\gamma}})}{\partial\vec{\gamma}} = \frac{P_2'Q - P_2Q'}{(\int_{\boldsymbol{R}_{\vec{\gamma}}}(I_x)^2\int_{\boldsymbol{R}_{\vec{\gamma}}}(I_y)^2 - (\int_{\boldsymbol{R}_{\vec{\gamma}}} I_xI_y)^2)^2}\vec{N} \qquad (3)$$

with

$$\begin{aligned}P_1 &= -\int_{\boldsymbol{R}_{\vec{\gamma}}}(I_y)^2\int_{\boldsymbol{R}_{\vec{\gamma}}} I_xI_t + \int_{\boldsymbol{R}_{\vec{\gamma}}} I_xI_y\int_{\boldsymbol{R}_{\vec{\gamma}}} I_yI_t \\ P_2 &= \int_{\boldsymbol{R}_{\vec{\gamma}}} I_xI_y\int_{\boldsymbol{R}_{\vec{\gamma}}} I_xI_t - \int_{\boldsymbol{R}_{\vec{\gamma}}}(I_x)^2\int_{\boldsymbol{R}_{\vec{\gamma}}} I_yI_t \\ Q &= \int_{\boldsymbol{R}_{\vec{\gamma}}}(I_x)^2\int_{\boldsymbol{R}_{\vec{\gamma}}}(I_y)^2 - (\int_{\boldsymbol{R}_{\vec{\gamma}}} I_xI_y)^2 \\ P_1' &= -(I_y)^2\int_{\boldsymbol{R}_{\vec{\gamma}}} I_xI_t - I_xI_t\int_{\boldsymbol{R}_{\vec{\gamma}}}(I_y)^2 \\ &\quad + I_xI_y\int_{\boldsymbol{R}_{\vec{\gamma}}} I_yI_t + I_yI_t\int_{\boldsymbol{R}_{\vec{\gamma}}} I_xI_y \\ P_2' &= I_xI_y\int_{\boldsymbol{R}_{\vec{\gamma}}} I_xI_t + I_xI_t\int_{\boldsymbol{R}_{\vec{\gamma}}} I_xI_y \\ &\quad -(I_x)^2\int_{\boldsymbol{R}_{\vec{\gamma}}} I_yI_t - I_yI_t\int_{\boldsymbol{R}_{\vec{\gamma}}}(I_x)^2 \\ Q' &= (I_x)^2\int_{\boldsymbol{R}_{\vec{\gamma}}}(I_y)^2 + (I_y)^2\int_{\boldsymbol{R}_{\vec{\gamma}}}(I_x)^2 - 2\,I_xI_y\int_{\boldsymbol{R}_{\vec{\gamma}}} I_xI_y\end{aligned}$$

The functional derivative $\frac{\partial\vec{u}(\boldsymbol{R}^c_{\vec{\gamma}})}{\partial\vec{\gamma}}$ of $\vec{u}(\boldsymbol{R}^c_{\vec{\gamma}})$ is obtained from these same expressions by replacing $\boldsymbol{R}_{\vec{\gamma}}$ with $\boldsymbol{R}^c_{\vec{\gamma}}$ and $\vec{N}$ by $-\vec{N}$. These functional derivatives completely specify the evolution Equation (1).

3. LEVEL SET REPRESENTATION

The descent equation (1) can be solved numerically by discretizing the interval $[0,1]$ of definition of $\vec{\gamma}$. This leads to an explicit reprentation of $\vec{\gamma}$, as with snakes [6], in terms of a number of points. However, a better alternative is to represent $\vec{\gamma}$ implicitly by the zero level set of a function $\phi : \Omega \mapsto \mathbb{R}$ with, by convention, $\phi > 0$ for points in the region inside $\vec{\gamma}$ and $\phi < 0$ for points in the region outside $\vec{\gamma}$. The curve $\vec{\gamma}$ itself is the zero level set of ϕ, i.e., $\vec{\gamma} = \{\boldsymbol{x} \in \Omega | \phi(\boldsymbol{x}) = 0\}$. This implicit level set representation of $\vec{\gamma}$ has several significant advantages over an explicit representation. An explicit representation can lead to large errors in the approximation of derivatives, as with the computation of curvature. Such errors do not occur with the level set implicit representation because the level set function is defined over the fixed grid of the image positional array. Also, an explicit curve representation does not allow for topology changes in the region enclosed by the curve; in particular, since the region enclosed by a simple curve in $\mathbb{R}^2$ is always connected and simply connected, an explicit curve representation does not allow a connected region to evolve into a disconnected region, or a simply connected region (i.e., a region "without holes") to evolve into a multiply connected region (i.e., a region "with holes"). In contrast, the implicit representation of curves as level sets of a function defined on Ω allows changes in the topology of the enclosed region. Another advantage of the level set representation is that region membership is explicit because points inside the region bounded by $\vec{\gamma}$ are the points where the level set function ϕ is positive, and those outside are the points where this function is negative. This information is not available explicitly with an explicit representation of $\vec{\gamma}$.

One can show that if the evolution of $\vec{\gamma}$ is defined by the equation

$$\frac{d\vec{\gamma}(s,\tau)}{d\tau} = F(\vec{\gamma}(s,\tau))\vec{N}(s,\tau)$$

where F is the 'speed' function defined over $\mathbb{R}^2$, then the corresponding evolution of the level set function ϕ is given by:

$$\frac{\partial \phi(\boldsymbol{x},\tau)}{\partial \tau} = F(\boldsymbol{x})\|\nabla \phi(\boldsymbol{x},\tau)\|$$

In our case, the speed function is given by the factor of $\vec{N}$ in the right-hand side of Equation (1) as specified by subsequents expressions in Section 2.2.

4. EXPERIMENTAL RESULTS

The two images at the top of Figure 1 are the two images of the sequence *Cosine* used in this first experiment. The intensity of the background (the ground), has been generated using the cosine function. The mask of the moving object (the figure), shown immediately below these two images, is a window cut out from, and superimposed on, the backgound. Between the two images, the figure moves diagonally down, one pixel in each direction. This is a simple example, ideal as a first experiment. The other images of Figure 1 show the evolution of an initial contour after the number of iterations given below each image.

The two images used in this second experiment are shown at the top of Figure 2. These are images of the *Aqua* sequence. The background (the ground) comes from a sequence of real images. The moving object (the figure) is the image of a fish and a portion of its background cut out from another sequence of real images. The figure moves diagonally, one pixel in each direction. The results of the algorithm, which determines a correct segmentation, are shown in Figure 2 by the evolution of an initial contour. These experiments demonstrate the feasibility and potential of the method, and justify a continuation of the study toward extensive experiments.

5. CONCLUSION

We proposed and described a novel algorithm for motion-based figure-ground segmentation based on the minimization of a functional for maximum separation between the motions of figure and ground. The Euler-Lagrange descent equations corresponding to the minimization of this functional are expressed as level set partial differential equations for a topology-free formulation and stable numerical implementation. These level set partial differential equations dictate the evolution of a surface whose zero level set at convergence is the desired figure ground segmentation. Preliminary results validate our proposed algorithm and demonstrate that accurate figure-ground segmentation based on motion alone and with no prior computation of motion can indeed be obtained.

6. REFERENCES

[1] S. Jehan-Besson, M. Barlaud, and G. Aubert, "Detection and tracking of moving objects using a new level set based method", in *Proc. Int. Conf. Pattern Recognition*, Barcelona, 2000.

[2] A.-R. Mansouri and J.Konrad, "Multiple Motion Segmentation with Level Sets", *IEEE Transactions on Image Processing*, 2002 (to appear).

[3] N. Paragios and R. Deriche, "Geodesic Active Contours and Level Sets for the Detection and Tracking of Moving Objects", *IEEE Transactions on Pattern Analysis and Machine Intelligence*, vol. 22, no.3, pp. 266-280, 2000.

[4] J. Sethian, "Level Set Methods : Evolving Interfaces in Geometry, Fluid Mechanics, Computer Vision, and Material Science", *Cambridge University Press*, 1996.

[5] A.Yezzi, A. Tsai, and A. Willsky, "A Fully Global Approach to Image Segmentation via Coupled Curve Evolution Equations" *Journal of Visual Communication and Image Representation*, vol. 13, no. 1/2, pp. 195-216, March/June 2002.

[6] M. Kass, A. Witkin, and D. Terzolpoulos, "Snakes: Active Contour Models," *International Journal of Computer Vision*, pp. 321-331, 1987.

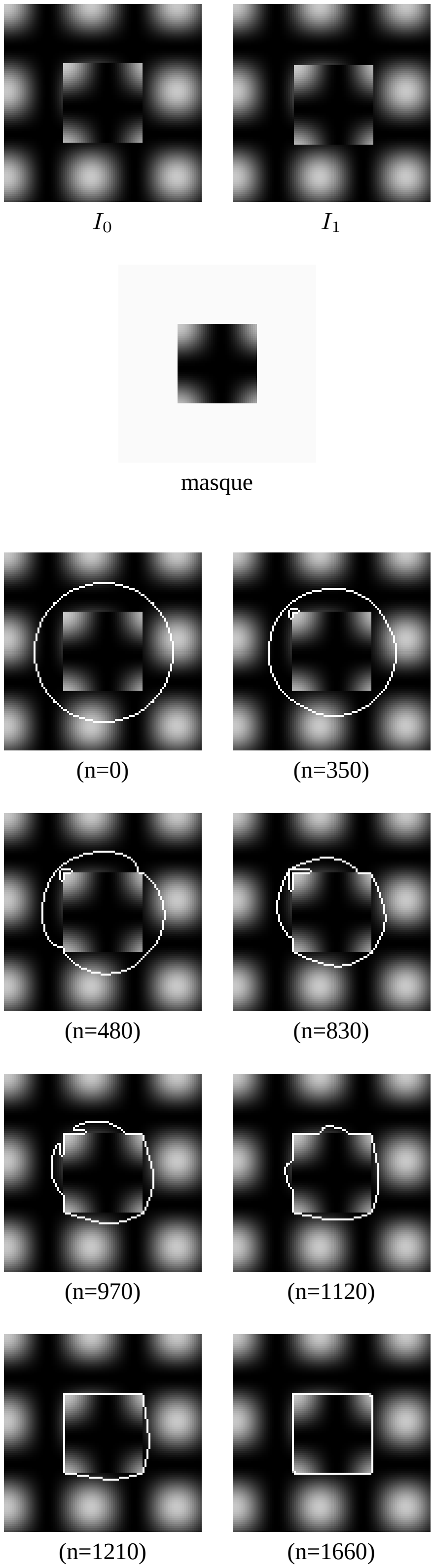

Fig. 1. Légende à compléter

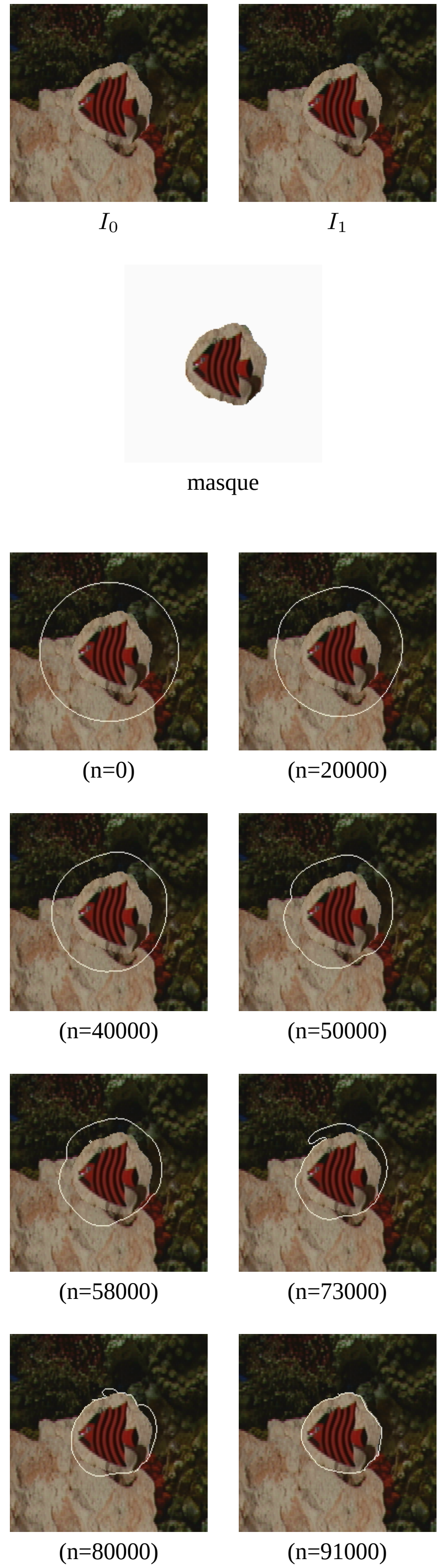

Fig. 2. Légende à compléter

In Proc. ICIP 2003, Sept. 14-17, 2003, Barcelona, Spain